AIAA JOURNAL
Vol. 48, No. 12, December 2010

Buckling and Static Analysis of Curvilinearly Stiffened Plates Using Mesh-Free Method

Ali Yeilaghi Tamijani* and Rakesh K. Kapania†
Virginia Polytechnic Institute and State University, Blacksburg, Virginia 24061

DOI: 10.2514/1.43917

With the advances being made in manufacturing technology, it is now possible to manufacture panels with arbitrary curvilinear stiffeners. A plate with curvilinear stiffeners can, in some cases, yield a desired structural response but with a lower mass. In this paper, the element-free Galerkin method is employed for buckling and static analysis of stiffened plates. The formulation allows the placement of any number of arbitrary curvilinear stiffeners within a plate. The first-order shear deformation theory is used to model the behavior of the plate and the stiffener. Moving-least-squares approximation is used to construct the shape functions. One of the major difficulties in the implementation of some mesh-free methods is the imposition of essential boundary conditions, as the approximations do not pass through the nodal parameter values. In this research, the penalty method is used for satisfying the boundary conditions. A mesh-free method frees the user from providing a nodal line on the plate along every stiffener. This is very beneficial for performing optimization studies. Several numerical examples using both straight and curvilinear stiffeners are obtained and compared with those available in the literature and those obtained using ANSYS®. This demonstrates the validity of the presented approach.

Nomenclature

A	=	area
b	=	stiffener binormal direction
D_p	=	plate stress–strain matrix for an isotropic material
D_s	=	stiffener stress–strain matrix for an isotropic material
$\det J$	=	Jacobian of the transformation
E	=	elastic modulus
F	=	force vector
h	=	thickness
I	=	second moment of the stiffener cross-sectional area
J_t	=	torsional stiffness of the stiffener
K	=	stiffness matrix
K_G	=	shear correction factor
K_{Gp}	=	plate geometric stiffness matrix
K_{Gs}	=	stiffener geometric stiffness matrix
ℓ	=	stiffener domain
N_i	=	shape function
n	=	stiffener normal direction
p	=	plate
S	=	centroidal distance of the stiffener to plate midsurface
s	=	stiffener
T_{sp}	=	transformation matrix relating the stiffener nodal displacements and the plate nodal displacements
t	=	stiffener tangential direction
U_p	=	plate strain energy
U_s	=	stiffener strain energy
u	=	displacement
$\bar{u}$	=	prescribed displacement
u_i	=	nodal displacements
W	=	potential of the membrane forces
w	=	deflection
$1/R$	=	curvature
α	=	angle between the stiffener tangential direction (t) and x axis
α_p	=	penalty parameter
Γ_t	=	prescribed tractions boundary
Γ_u	=	prescribed displacements boundary
ε_p	=	plate strain vector
ε_s	=	stiffener strain vector
ε_{Gp}	=	plate nonlinear strain vector
ε_{Gs}	=	stiffener nonlinear strain vector
ζ	=	natural coordinate
θ_n	=	stiffener rotation with respect to t direction
θ_t	=	stiffener rotation with respect to n direction
Λ	=	coordinate transformation matrix
λ	=	buckling parameter
λ_b	=	buckling load factor
σ_t	=	stiffener axial stress
τ_{Gp}	=	plate stress vector
υ	=	Poisson's ratio
Π	=	potential energy
φ_{px}	=	plate rotation with respect to y axis
φ_{py}	=	plate rotation with respect to x axis
φ_{sx}	=	stiffener rotation with respect to y axis
φ_{sy}	=	stiffener rotation with respect to x axis
Ω	=	plate domain

Presented as Paper 2009-2454 at the 50th AIAA/ASME/ASCE/AHS/ASC Structures, Structural Dynamics, and Materials Conference, Palm Springs, CA, 4–7 May 2009; received 18 February 2009; revision received 15 June 2010; accepted for publication 16 June 2010.

*Ph.D. Candidate, Department of Engineering Science and Mechanics; ayt@vt.edu. Member AIAA.

†Mitchell Professor, Department of Aerospace and Ocean Engineering; rkapania@vt.edu. Associate Fellow AIAA.

I. Introduction

STIFFENED-PLATE structures are very common in engineering and are used in aerospace and ship building due to their very high stiffness-to-weight ratio. The stiffeners are designed to meet the strength or stiffness requirements of a particular situation. The stability of these structures is of great interest, since it generally controls the optimum design of the structures in which they are deployed. Also, only a comprehensive and accurate stress analysis can lead a designer to an appropriate selection of the plate thickness distribution and the stiffener dimensions.

The study of stability of stiffened plates has a long history. The widespread application of stiffened plates has resulted in different methods for performing an appropriate structural analysis of these plates. A large number of studies on bending, buckling, and vibration of stiffened panels are available in the literature. Timoshenko and Gere [1] presented numerical tables for buckling loads of rectangular plates stiffened by longitudinal and transverse ribs. The effect of

eccentricity of the stiffeners on the stress–strain matrix was introduced by modifying the second moment of area of the stiffener by Seide [2]. Kolakowski [3] presented a semi-analytical method for the buckling analysis including modal interaction of prismatic plate structures using trigonometric series. A semi-analytical model for global buckling and postbuckling analysis of stiffened panels was proposed by Byklum et al. [4]. In their research, the loads were biaxial in-plane compression or tension, shear, and lateral pressure. By using the principle of virtual work and assuming deflections in the form of trigonometric function series, they solved the buckling and postbuckling analysis of stiffened panels. Perturbation methods were used for solving the nonlinear algebraic equilibrium equations that are generated by the principle of virtual work.

Brubak et al. [5] presented a semi-analytical model for buckling strength analysis of stiffened plates with arbitrarily oriented stiffeners. By using the proposed model, a stiffened plate with different boundary conditions can be modeled. In the strain energy formulations, which are considered in their research, the coupling terms between bending and membrane components for the plate and stiffeners were ignored. Later, Bedair [6] discussed that since there are other several papers on the buckling of stiffened plates available in the literature, Brubak et al. [5] should have compared the efficiency of their formulations to some of these methods, since they had claimed that theirs is an efficient method. Bedair [6] also discussed that the authors ignored the contribution of torsional rigidity of the stiffeners in their formulations and pointed out that Brubak et al. [5] should have mentioned that this assumption is not valid for the stiffeners with closed sections. The lack of stating the assumptions relating the displacements of the stiffeners to the midplane displacements of the plate, ignoring the coupling terms between bending and membrane components for the plate and stiffeners and comparing the computer speed of their solution to the ANSYS® were also discussed by Bedair [6].

Several finite element models are developed to analyze buckling of stiffened plate. Shastry et al. [7] studied finite element model for the plate and stiffener and applied it to the stability analysis of stiffened plates subjected to arbitrary in-plane loading. Mukhopadhyay and Mukherjee [8] applied the finite element model for the buckling analysis of the stiffened plates. The stiffened plate was modeled by using isoparametric bending element. In their formulation, the stiffener nodes need not to be necessarily connected to those of the plate and they can be located anywhere within the plate element. The element developed by Mukhopadhyay and Mukherjee is an isoparametric quadratic element and has the advantages that it can represent irregular boundaries and laminated plates and can account for shear deformations.

Biswal and Ghosh [9] developed a four-noded rectangular element with seven degrees of freedom at each node for a laminated plate. They used a higher-order shear deformation theory, which can explain the parabolic distribution of transverse shear stresses and the nonlinearity of the in-plane displacements across the thickness. The stiffness of the stiffener is reflected at all four nodes of the plate element in which it is located. However, in Biswal and Ghosh's paper, the stiffener element can be placed parallel to the x or y directions only. The stiffness matrix of a stiffened-plate element consists of the contributions of the plate and that of the stiffeners. A nine-noded plate element and a three-noded stiffener element were developed by Sadek and Tawfik [10] to model the stiffened composite plates. The model is based on a higher-order shear deformation theory, which is derived out of a power series expansion of the midsurface displacements. The model is applicable for both moderately thick and thin stiffened composite plates. By using the transformation matrix, the stiffener nodal parameters transform to the plate nodal parameters. Consequently, the stiffeners can be positioned anywhere within the plate element along lines of constant natural coordinates and need not necessarily be placed on the plate nodes.

Guot and Lindner [11] developed a material and geometric nonlinear spline strip method to analyze the stiffened panels subjected to axial compression. They mentioned that since the collapse of stiffened panel made of thin steel plates is often caused by the interaction between the local buckling of the plate and stiffeners and the overall buckling of the whole stiffened panel, they studied the elastic-plastic interaction behavior of the stiffened panel. Kirchhoff hypothesis was used to model both the plate and the beam. The residual stresses and initial geometric imperfections are considered and their effects on the ultimate strength of the stiffened panel were considered.

As mentioned earlier, many methods have been implemented for the buckling and stress problems. These methods include analytical and numerical techniques, such as the Ritz method, the finite strip methods and the finite element method (FEM). The most common method is finite element method, which has become the numerical method of choice in structural mechanics due to its versatility and many powerful commercial software packages that are available now. However, the existences of some difficulties, e.g., distorted elements, in the FEM sometimes cause error in the results.

To avoid meshing, a tedious and time consuming affair, of a domain using finite elements, meshless methods are increasingly being used to solve problems in solid mechanics. In the mesh-free methods, the displacement approximation is defined based on a set of particles in the influence domain. Various approaches have been proposed in the literature. Two of these approaches are the element-free Galerkin (EFG) [12] using moving least-squares (MLS) and the meshless local Petrov–Galerkin (MLPG) [13] using MLS or symmetric smoothed particle hydrodynamics (SSPH) [14].

Krysl and Belytschko [12] presented meshless approach to the analysis of the arbitrary Kirchhoff shells by the EFG method. The shell theory used is geometrically exact and can be applied to deep shells. The method is based on moving-least-squares approximant. The element-free Galerkin method is almost identical to the conventional FEM, as both of them are based on the Galerkin formulation, and employ local interpolation/approximation to approximate the trial functions. The key differences lie in the interpolation methods, integration schemes and in the enforcement of essential boundary conditions. Atluri and Zhu [13] proposed an MLPG method, which is a truly meshless method. Remarkable successes of MLPG method have been reported in solving convection diffusion problems, fracture mechanics problems, and shell and plate bending problems.

Batra and Zhang [14] proposed a new and simple technique called the symmetric smoothed particle hydrodynamics method to construct basis functions for meshless methods that use only locations of particles. The idea is based on approximating derivatives of a function without differentiating the basis functions. By using Taylor series the function is related to neighboring nodes. In this method, the restrictions on the choice of the kernel function are fewer than those for other smoothed particle hydrodynamics methods. Consequently, it is possible to use a wider class of kernel functions. They used their proposed basis functions for constructing the strong and a weak form of equations of equilibrium for a 2-D elastic problem.

Peng et al. [15,16] used the EFG method for the static and buckling analysis of concentrically and eccentrically stiffened plates. They used first-order shear deformation theory to model the plate and stiffeners. It has been shown in their papers that by using the EFG method, Peng et al. avoided the need for remeshing that occurs with FEM because the stiffeners need to be placed along the mesh lines or plate element and the change of the stiffener position leads to remeshing of the entire plate domain.

Kapania and Li [17,18] studied the geometrically exact finite strain curved twisted beam theory with large displacements/rotations and extended using orthonormal frames and the rigid-cross-section assumption. Except for the rigid-cross-section assumption, no further approximations were made in the formulations. All reference frames are orthonormal and therefore the geometric aspects become more direct. They used the principle of virtual work to derive the equations for initially curved/twisted beams by considering the first Piola–Kirchhoff stresses. The developed formulation can be used for 3-D natural curved/twisted slender beams with finite strains and rotations. Several examples for slender beam cases were presented to test the developed element formulation. Since the initial curvature

correction term is considered by Kapania and Li, especially when long-term dynamic responses are concerned, their formulation may give more accurate results.

The present authors developed the element-free Galerkin method for vibration analysis of the plate with curvilinear stiffeners. They showed the effect of stiffener's location and curvature on the natural frequencies, mode shapes, and frequency response [19]. This paper presents the EFG method for the buckling and stress analysis of the plate with curvilinear stiffener. The stiffener cross section is assumed to be symmetric about the stiffener binormal axis and the stiffener is assumed to remain perpendicular to the plate during deformation. The plate and stiffener are modeled using the first-order shear deformation theory (FSDT). The determination of the buckling load and the stress analysis of panels with curvilinear stiffeners using meshless method, to the authors' knowledge, has not previously appeared. Moving-least-squares approach is used for developing the shape functions for analyzing the stiffened plate. One of the problems with the MLS approximants is that, in general, they do not pass through the data used to fit the curve. Therefore, the essential boundary conditions in the EFG methods cannot be easily and directly enforced. Several approaches have been studied for enforcing the essential boundary conditions in the EFG method, such as the direct collocation method, Lagrange multipliers method, and the penalty method. The essential boundary conditions in the present formulation are imposed by the penalty method.

In the developed approach, the stiffeners need not necessarily be placed on the particles' lines of the plate, and the location and the number of particles for the stiffener representation can be modified without changing the same for the plate. This has been achieved through the transformation of stiffener displacement related parameters to those of the plate. The elements and their connectivity required for the FEM are avoided. Only an array of scattered nodes in the domain under consideration is required for the approximation. Thus, the current approximation technique suggested in the companion paper [19] is flexible. The number and location of nodes can be chosen freely. Consequently, there is no limitation on the curvature and location of a stiffener.

In the sections that follow, first the potential energy for the plate and stiffener will be described. Then the formulation of the meshless method for analyzing buckling and static analysis of stiffened plate will be developed. In the developed formulation for buckling analysis, the local buckling is ignored by limiting the stiffeners slenderness. The formulation is based on EFG. Several examples of rectangular stiffened plates with different stiffeners have been presented. The effect of eccentricity and concentricity is also studied in different examples. The developed method results are compared with the results that are available in the literature and with those obtained using ANSYS software.

II. Formulation of the Problem

A. Potential Energy of the Plate

In this paper, the MLS technique is used for displacement approximation. Using MLS basis function, the displacement can be explained as

$$u^h = \sum_{i=1}^{n} N_i(X)\hat{u}_i \tag{1}$$

where $\hat{u}_i$ is the nodal parameters and $N_i(X)$ is the shape function, which is defined in [19]. The shape of the influence domain of X can be a square or a circle. In this paper, square domains are used. The weight functions play an important role in MLS approximation. Several weight functions are available in the literature. In this research, the spline weight function, which is defined in [19], is employed that satisfies the continuity of the weight function as well as its first and second derivatives.

The strain energy of the plate U_p is defined in the Appendix. For the buckling analysis, the bending moments developed due to the action of in-plane loads are considered. Thus, the nonlinear terms in strain-displacement relations are considered. in-plane displacements have not been taken into account for the formation of geometric stiffness matrices, as they would increase the complexity of the formulation without any significant improvement in results [8]. The nonlinear terms in the plate strain terms are [8]

$$\varepsilon_{Gp} = \begin{Bmatrix} \frac{1}{2}\left(\frac{\partial w}{\partial x}\right)^2 + \frac{z^2}{2}\left(\frac{\partial \varphi_{px}}{\partial x}\right)^2 + \frac{z^2}{2}\left(\frac{\partial \varphi_{py}}{\partial x}\right)^2 \\ \frac{1}{2}\left(\frac{\partial w}{\partial y}\right)^2 + \frac{z^2}{2}\left(\frac{\partial \varphi_{px}}{\partial y}\right)^2 + \frac{z^2}{2}\left(\frac{\partial \varphi_{py}}{\partial y}\right)^2 \\ \left(\frac{\partial w}{\partial x}\right)\left(\frac{\partial w}{\partial y}\right) + z^2\left(\frac{\partial \varphi_{px}}{\partial x}\right)\left(\frac{\partial \varphi_{px}}{\partial y}\right) + z^2\left(\frac{\partial \varphi_{py}}{\partial x}\right)\left(\frac{\partial \varphi_{py}}{\partial y}\right) \end{Bmatrix} \tag{2}$$

where w is the displacement components along the z directions, φ_{px} and φ_{py} are the rotations with respect to the y and x axis and p indicates the plate (Fig. 1). Equation (2) can be written as

$$\varepsilon_{Gp} = \tfrac{1}{2}[A_p][H_p]\{\varepsilon_{Np}\}$$

where

$$[A_p] = \begin{bmatrix} \frac{\partial w}{\partial x} & 0 & z\frac{\partial \varphi_{px}}{\partial x} & 0 & z\frac{\partial \varphi_{py}}{\partial x} & 0 \\ 0 & \frac{\partial w}{\partial y} & 0 & z\frac{\partial \varphi_{py}}{\partial y} & 0 & z\frac{\partial \varphi_{px}}{\partial y} \\ \frac{\partial w}{\partial y} & \frac{\partial w}{\partial x} & z\frac{\partial \varphi_{px}}{\partial y} & z\frac{\partial \varphi_{py}}{\partial x} & z\frac{\partial \varphi_{py}}{\partial y} & z\frac{\partial \varphi_{px}}{\partial x} \end{bmatrix}$$

$$[H_p] = \begin{bmatrix} 1 & & & & & \\ 0 & 1 & & & \text{sym.} & \\ 0 & 0 & z & & & \\ 0 & 0 & 0 & z & & \\ 0 & 0 & 0 & 0 & z & \\ 0 & 0 & 0 & 0 & 0 & z \end{bmatrix} \tag{4}$$

and

$$\varepsilon_{Np} = \begin{bmatrix} \frac{\partial w}{\partial x} & \frac{\partial w}{\partial y} & \frac{\partial \varphi_{px}}{\partial x} & \frac{\partial \varphi_{py}}{\partial y} & \frac{\partial \varphi_{py}}{\partial x} & \frac{\partial \varphi_{px}}{\partial y} \end{bmatrix}^T \tag{5}$$

The potential of the membrane forces in the plate is given by

$$W_p = -\int_V \varepsilon_{Gp}^T \tau_{Gp}\, \mathrm{d}V \tag{6}$$

where

$$\tau_{Gp} = \begin{Bmatrix} \sigma_x \\ \sigma_y \\ \tau_{xy} \end{Bmatrix} \tag{7}$$

It can be shown that the potential of the membrane force can be written as [20]

$$W_p = -\frac{1}{2}\int_A \varepsilon_{Np}^T \sigma_p \varepsilon_{Np}\, \mathrm{d}A \tag{8}$$

where

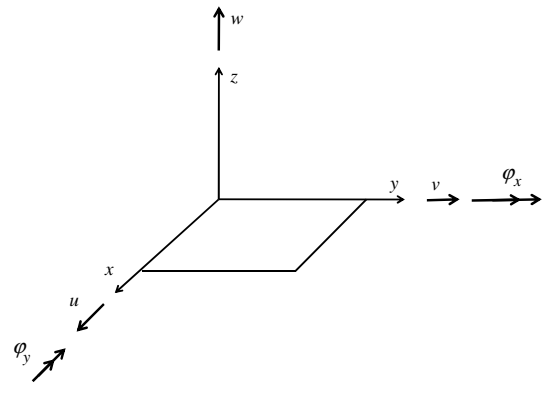

Fig. 1 Directions of the generalized displacements of the plate.

$$\sigma_p = \begin{bmatrix} \sigma_x h & & & & & \\ \tau_{xy} h & \sigma_y h & & & & \\ 0 & 0 & \frac{h^3}{12}\sigma_x & & \text{sym.} & \\ 0 & 0 & 0 & \frac{h^3}{12}\sigma_y & & \\ 0 & 0 & 0 & \frac{h^3}{12}\tau_{xy} & \frac{h^3}{12}\sigma_x & \\ 0 & 0 & \frac{h^3}{12}\tau_{xy} & 0 & 0 & \frac{h^3}{12}\sigma_y \end{bmatrix} \tag{9}$$

By using Eq. (1), Eq. (5) can be written as

$$\varepsilon_{Np} = B_{Np}\delta_p \tag{10}$$

where B_{Np} is defined in the Appendix. By substituting Eq. (10) in Eq. (8),

$$W_p = -\frac{1}{2}\delta_p^T \int_A B_{Np}^T \sigma_p B_{Np}\, \mathrm{d}A\, \delta_p \tag{11}$$

where δ_p is given in the Appendix.

B. Potential Energy of a Stiffener

The strain energy of the plate U_s is defined in the companion paper [19]. The nonlinear part of the stiffener strain is

$$\varepsilon_{Gs} = \frac{1}{2}\left(\frac{1}{\det J}\frac{\mathrm{d}w}{\mathrm{d}\zeta}\right)^2 + \frac{z^2}{2}\left(\frac{1}{\det J}\frac{\mathrm{d}\theta_t}{\mathrm{d}\zeta} + \frac{\theta_n}{R(\zeta)}\right)^2 + \frac{z^2}{2}\left(\frac{1}{\det J}\frac{\mathrm{d}\theta_n}{\mathrm{d}\zeta} - \frac{\theta_t}{R(\zeta)}\right)^2 \tag{12}$$

where $\det J$ is the Jacobian of the transformation; $R(\zeta)$ is the radius of curvature (Fig. 2a); ζ is the natural coordinate for parameterizing the curve (Fig. 2c), which are described in [19]; and θ_t, θ_n, and w, which are the rotations and deflection, are shown in Fig. 2b. Equation (12) can be written as

$$\varepsilon_{Gs} = \frac{1}{2}[A_s][H_s]\{\varepsilon_{Ns}\} \tag{13}$$

where

$$[A_s] = \begin{bmatrix} \frac{1}{\det J}\frac{\mathrm{d}w}{\mathrm{d}\zeta} & z\left(\frac{1}{\det J}\frac{\mathrm{d}\theta_t}{\mathrm{d}\zeta} + \frac{\theta_n}{R(\zeta)}\right) & z\left(\frac{1}{\det J}\frac{\mathrm{d}\theta_n}{\mathrm{d}\zeta} - \frac{\theta_t}{R(\zeta)}\right) \end{bmatrix}$$

$$[H_s] = \begin{bmatrix} 1 & & \text{sym.} \\ 0 & z & \\ 0 & 0 & z \end{bmatrix} \tag{14}$$

and

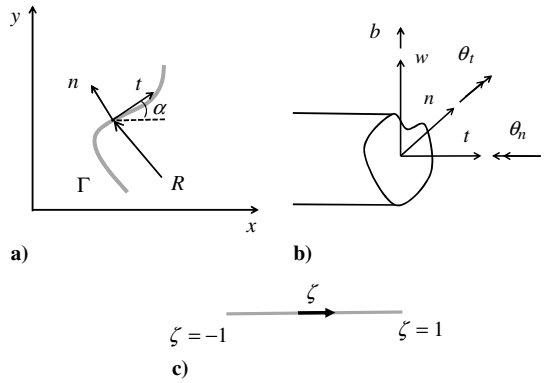

Fig. 2 Plots of a) local and global coordinate systems for curvilinear stiffener, b) directions of the generalized displacements of the stiffener, and c) transformed plane of curvilinear stiffener.

$$\varepsilon_{Ns} = \begin{bmatrix} 0 & 0 & \frac{1}{\det J}\frac{\mathrm{d}}{\mathrm{d}\zeta} \\ \frac{1}{\det J}\frac{\mathrm{d}}{\mathrm{d}\zeta} & \frac{1}{R(\zeta)} & 0 \\ -\frac{1}{R(\zeta)} & \frac{1}{\det J}\frac{\mathrm{d}}{\mathrm{d}\zeta} & 0 \end{bmatrix} \begin{Bmatrix} \theta_t \\ \theta_n \\ w \end{Bmatrix} = L_{Ns} u_s' \tag{15}$$

The potential of the membrane forces in the stiffener is given by

$$W_s = -\int_V \varepsilon_{Gs}\sigma_t\, \mathrm{d}V \tag{16}$$

where σ_t is the axial stress of the stiffener. It can be shown that [20]

$$W_s = -\frac{1}{2}\int_{-1}^{1} \varepsilon_{Ns}^T \sigma_s \varepsilon_{Ns} \det J\, \mathrm{d}\zeta \tag{17}$$

where

$$\sigma_s = \begin{bmatrix} \sigma_t A & 0 & 0 \\ 0 & \sigma_t I_n & 0 \\ 0 & 0 & \sigma_t I_n \end{bmatrix} \tag{18}$$

In the above equation, A is the cross-sectional areas, and I_n is the second moment of the stiffener cross-sectional area about the reference axis. The displacement fields in terms of global coordinate system are

$$u_s' = \begin{Bmatrix} u_t \\ v_n \\ \theta_t \\ \theta_n \\ w_s \end{Bmatrix} = \begin{bmatrix} \cos\alpha & \sin\alpha & 0 & 0 & 0 \\ -\sin\alpha & \cos\alpha & 0 & 0 & 0 \\ 0 & 0 & \cos\alpha & \sin\alpha & 0 \\ 0 & 0 & -\sin\alpha & \cos\alpha & 0 \\ 0 & 0 & 0 & 0 & 1 \end{bmatrix} \begin{Bmatrix} u_{s_0} \\ v_{s_0} \\ \varphi_{sx} \\ \varphi_{sy} \\ w_{s_0} \end{Bmatrix} = \Lambda u_s \tag{19}$$

where u_{s_0}, v_{s_0}, and w_{s_0} are the midplane displacements along the x, y, and z directions, respectively; φ_{sx} and φ_{sy} are the rotations with respect to the y and x axis, respectively; and α is the angle between the t and x axes (Fig. 2a). By using Eqs. (1), (15), and (19), the strain in global coordinate system can be written as

$$\varepsilon_{Ns} = B_{Ns}\Lambda\delta_s \tag{20}$$

where B_{Ns} and δ_s are given in the Appendix. Substituting Eq. (20) in Eq. (17), the potential of the membrane forces of a stiffener can be written as

$$W_s = -\frac{1}{2}\delta_s^T \int_{-1}^{1} \Lambda^T B_{Ns}^T \sigma_s B_{Ns} \Lambda \det J\, \mathrm{d}\zeta\, \delta_s \tag{21}$$

The stiffener particle parameters can be presented as the plate particle parameters by using a transformation matrix (see [19] for details):

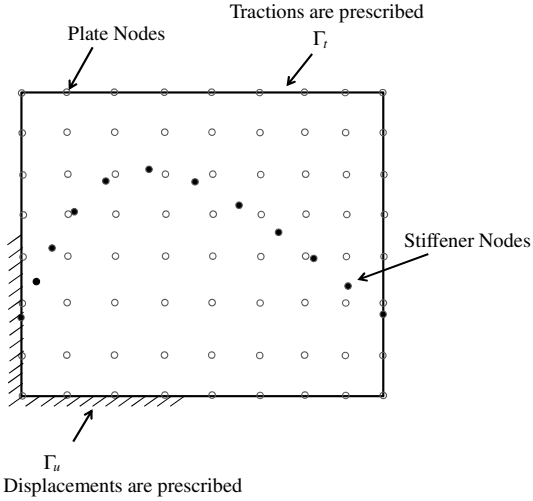

Fig. 3 Prescribed boundaries of the plate with a curvilinear stiffener.

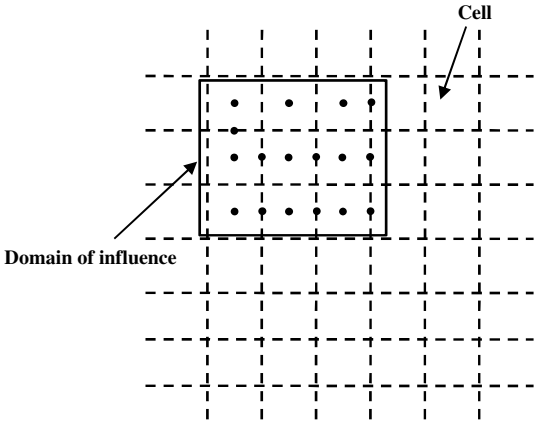

Fig. 4 Domain of influence and background cell structures.

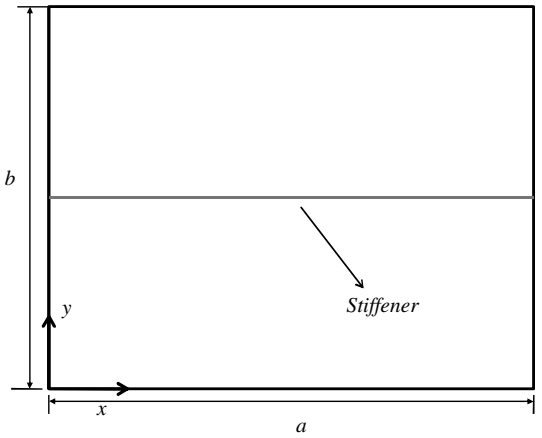

Fig. 5 Plate with a single stiffener.

$$\delta_s = T_{sp}\delta_p \tag{22}$$

where T_{sp} is the transformation matrix [19].

C. Enforcement of Essential Boundary Conditions

A drawback of the EFG methods, using the MLS basis function, lies in that they do not allow a direct imposition of the essential boundary conditions [21]. Earlier works have employed Lagrange multipliers or modified variational principle for this purpose. Recently, a singular weight function, which allows the direct imposition of essential boundary conditions, was tested while retaining a high degree of efficiency and accuracy. This method does not satisfy the essential boundary conditions exactly. Instead, it converges to the exact essential boundary conditions as nodal refinement on the boundary is increased. Another method that is common in the finite element as well as mesh-free methods is the penalty method. In the present formulation, this method is implemented. The boundary conditions are shown in Fig. 3. By using the potential of the membrane forces (W_p and W_s) and the strain energy (U_p and U_s) of the plate and stiffener, the total potential energy can be defined as

$$\Pi = U_p + U_s + W_p + W_s - \int_{\Gamma_t} u^T f \,\mathrm{d}\Gamma + \frac{\alpha_p}{2}\int_{\Gamma_u} (u-\bar{u})^T (u-\bar{u})\,\mathrm{d}\Gamma \tag{23}$$

where $\bar{u}$ and f are prescribed displacement and traction on the boundaries. An important consideration for using the penalty method is the choice of an appropriate penalty parameter α_p. We should note that the penalty terms will not only affect the diagonal entries of the system stiffness matrix but also the offdiagonal entries of the system matrix. The system stiffness matrix may become ill conditioned when the offdiagonal entries are multiplied by a very large number. From literature review [21], the penalty parameter can be chosen as $(10^3 - 10^7) \times E$, where E is the Young's modulus of the material under consideration.

D. Derivation of the Stiffness Matrices and the Force Vector for Static Analysis

In the formulation of linear element-free Galerkin method for static analysis, it is assumed that deformations remain small so that linear relations can be used to represent the strain in a body. The emphasis of this section is on developing a formulation for the static analysis of the stiffened plates. Since the nonlinear part of strain is neglected in the static analysis, Eq. (23) can be rewritten as

$$\Pi_{\mathrm{st}} = U_p + U_s - \int_{\Gamma_t} u^T f \,\mathrm{d}\Gamma + \frac{\alpha_p}{2}\int_{\Gamma_u} (u-\bar{u})^T (u-\bar{u})\,\mathrm{d}\Gamma \tag{24}$$

By substituting Eq. (A1) in Eq. (24) and using the variation of the potential energy (Π_{st}), the mathematical model for the static analysis stiffened plate is found to be

$$\delta\left(\delta_p^T\left(\frac{1}{2}\left(\int_A B_p^T D_p B_p \,\mathrm{d}A + T_{sp}^T \int_{-1}^{1} \Lambda^T B_s^T D_s B_s \Lambda \det J \,\mathrm{d}\zeta T_{sp} + \alpha_p \int_{\Gamma_u} N_p^T N_p \,\mathrm{d}\Gamma\right)\delta_p - \alpha_p \int_{\Gamma_u} N_p^T \bar{u}\,\mathrm{d}\Gamma - \int_{\Gamma_t} N_p^T f \,\mathrm{d}\Gamma\right)\right) = 0 \tag{25}$$

where B_p, B_s, D_p, and D_s are defined in the Appendix. Solving the above equation will result in equilibrium equation:

$$(K_p + K_s)\,\delta_p = F \tag{26}$$

where K_p, K_s, and F are defined in the Appendix.

In the integration in Eq. (A6), the stiffness matrices and the force vector are performed numerically over a cell structure that is composed of rectangles (Fig. 4). Additionally, a higher-order Gaussian integration scheme may be required for integration over each cell to obtain accurate results [19]. The global coordinates of an integration point are determined through a mapping of their local coordinates using Lagrange shape functions and the coordinates of the integration cells' vertices. For problems with a rectangular geometry, rectangular integration cells map the problem domain exactly. For curved geometries, depending on the level of refinement of the integration cells, such integration cells may lead to a small discretization error [21].

E. Derivation of the Geometric Stiffness Matrices for Buckling Analysis

For conducting the buckling analysis, the nonlinear terms in the strain will be considered. The equation for the stability problem can be obtained by defining the total potential energy as

Table 1 Buckling parameters for rectangular stiffened plates with varying stiffener rigidity

δ	Timoshenko and Gere [1]	Mukhopadhyay and Mukherjee [8]	Mesh-free
		$\gamma = 5$	
0.05	12	11.72	11.71
0.1	11.1	10.93	10.94
0.2	9.72	9.7	9.61
		$\gamma = 10$	
0.05	16	16	15.85
0.1	16	16	15.86
0.2	15.8	15.44	15.37
		$\gamma = 15$	
0.05	16	16	15.86
0.1	16	16	15.86
0.2	16	16	15.87

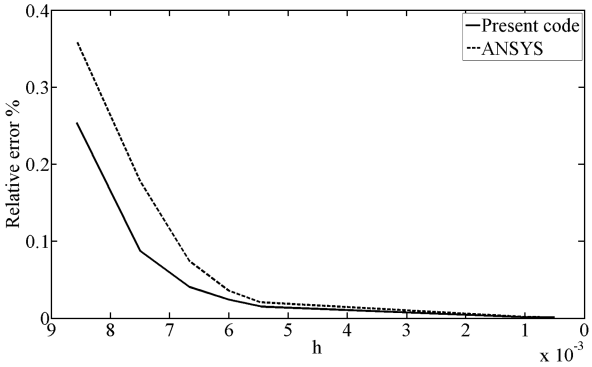

Fig. 6 Relative error in buckling parameter using mesh-free methods and ANSYS.

$$\Pi_G = U_p + U_s + W_p + W_s + \frac{\alpha_p}{2}\int_{\Gamma_u}(u-\bar{u})^T(u-\bar{u})\,\mathrm{d}\Gamma \quad (27)$$

By using the variation of the potential energy Π_G,

$$\delta\Bigg(\delta_p^T\Bigg(\Bigg(\frac{1}{2}\Bigg(\int_A B_p^T D_p B_p\,\mathrm{d}A + T_{sp}^T\int_{-1}^{1}\Lambda^T B_s^T D_s B_s \Lambda\det J\,\mathrm{d}\zeta T_{sp} + \alpha_p\int_{\Gamma_u} N_p^T N_p\,\mathrm{d}\Gamma\Bigg) - \int_A B_{Np}^T\sigma_p B_{Np}\,\mathrm{d}A - T_{sp}^T\int_{-1}^{1}\Lambda^T B_{Ns}^T\sigma_s B_{Ns}\Lambda\det J\,\mathrm{d}\zeta\, T_{sp}\Bigg)\delta_p - \alpha_p\int_{\Gamma_u} N_p^T\bar{u}\,\mathrm{d}\Gamma\Bigg)\Bigg) = 0 \quad (28)$$

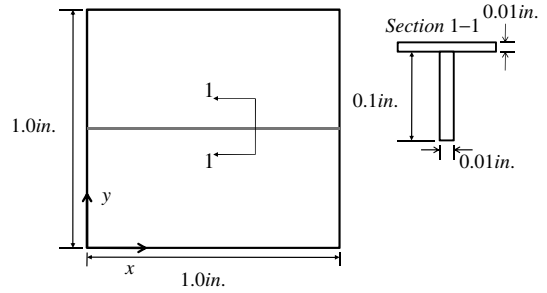

Fig. 7 Simply supported square plate stiffened centrally by one stiffener.

The above equation will give the linear eigenvalue problem:

$$K_p + K_s - \lambda_b(K_{Gp} + K_{Gs}) = 0 \quad (29)$$

where K_{Gs} and K_{Gp} are the assembled geometric stiffness matrices for stiffeners and plate, respectively. They are defined in the Appendix. Assuming that K_{Gs} and K_{Gp} are initially positive definite and varies gradually during a loading process, the buckling load factor λ_b can be detected using eigenvalue analysis.

III. Results and Discussion

To demonstrate the versatility and to validate the method, buckling analysis of several plates with different stiffeners, both straight and curvilinear, are carried out and the results are compared with the existing ones or with those obtained using ANSYS, a commercially available software. Generally speaking, this method is applicable to plates with different kinds of stiffeners. The selected examples are for

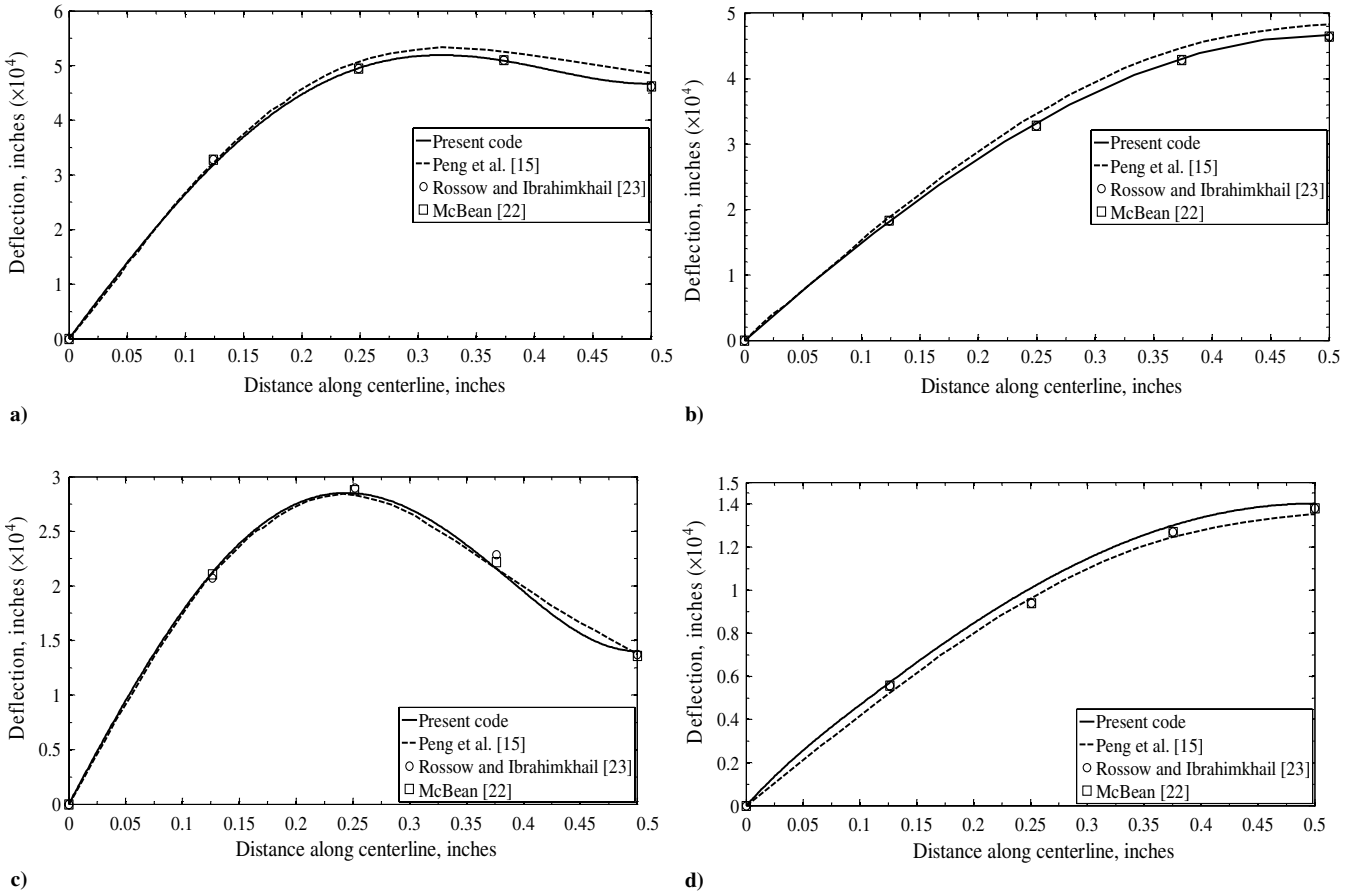

Fig. 8 Deflection along centerline: a) $x = 0.5$ in., b) $y = 0.5$ in. of the concentrically stiffened plate, c) $x = 0.5$ in., and d) $y = 0.5$ in. of the eccentrically stiffened plate.

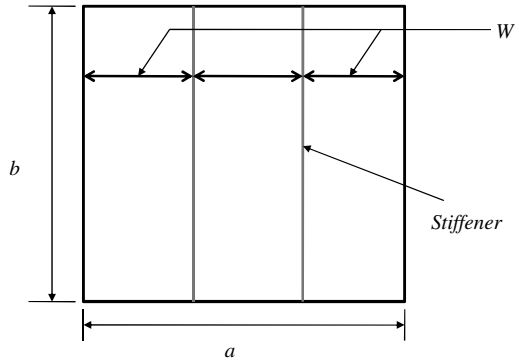

Fig. 9 Square plate with double stiffeners.

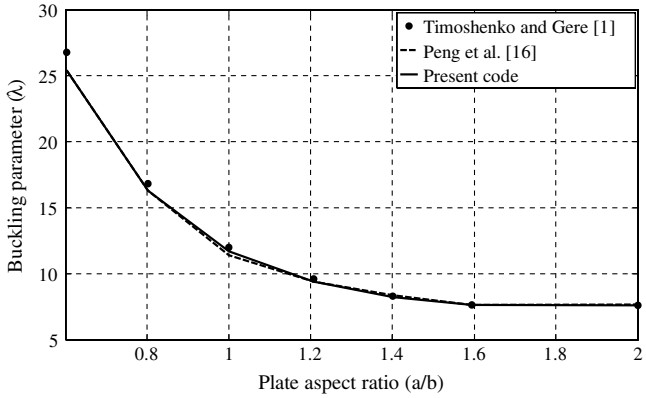

Fig. 10 Buckling parameter of plate stiffened by two stiffeners for different plate aspect ratios.

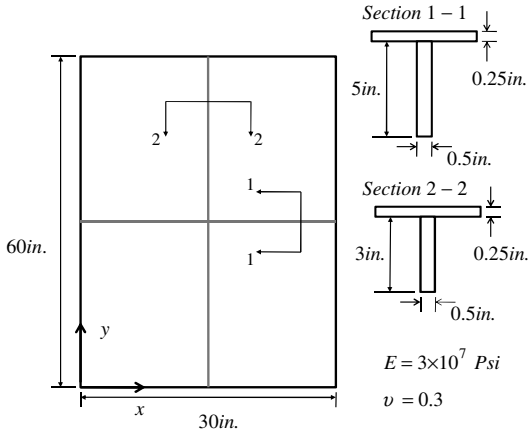

Fig. 11 Rectangular plate stiffened by two stiffeners.

comparison purpose only and do not represent the full capabilities of the proposed method. A rectangular domain is considered and the scaling factor of 4, in both x and y directions, for all examples is used (see [15] for details). To evaluate the integrals in all equations over each cell, the Gauss integration rule with 16 integration points in each cell are used.

A. Simply Supported Plate with a Single Stiffener

First, the buckling analysis of a series rectangular plate simply supported on all four edges and with one central stiffener has been considered as shown in Fig. 5. The plate is under uniaxial in-plane compression in the x direction. The results are compared with those available in Timoshenko and Gere [1]. Mukhopadhyay and

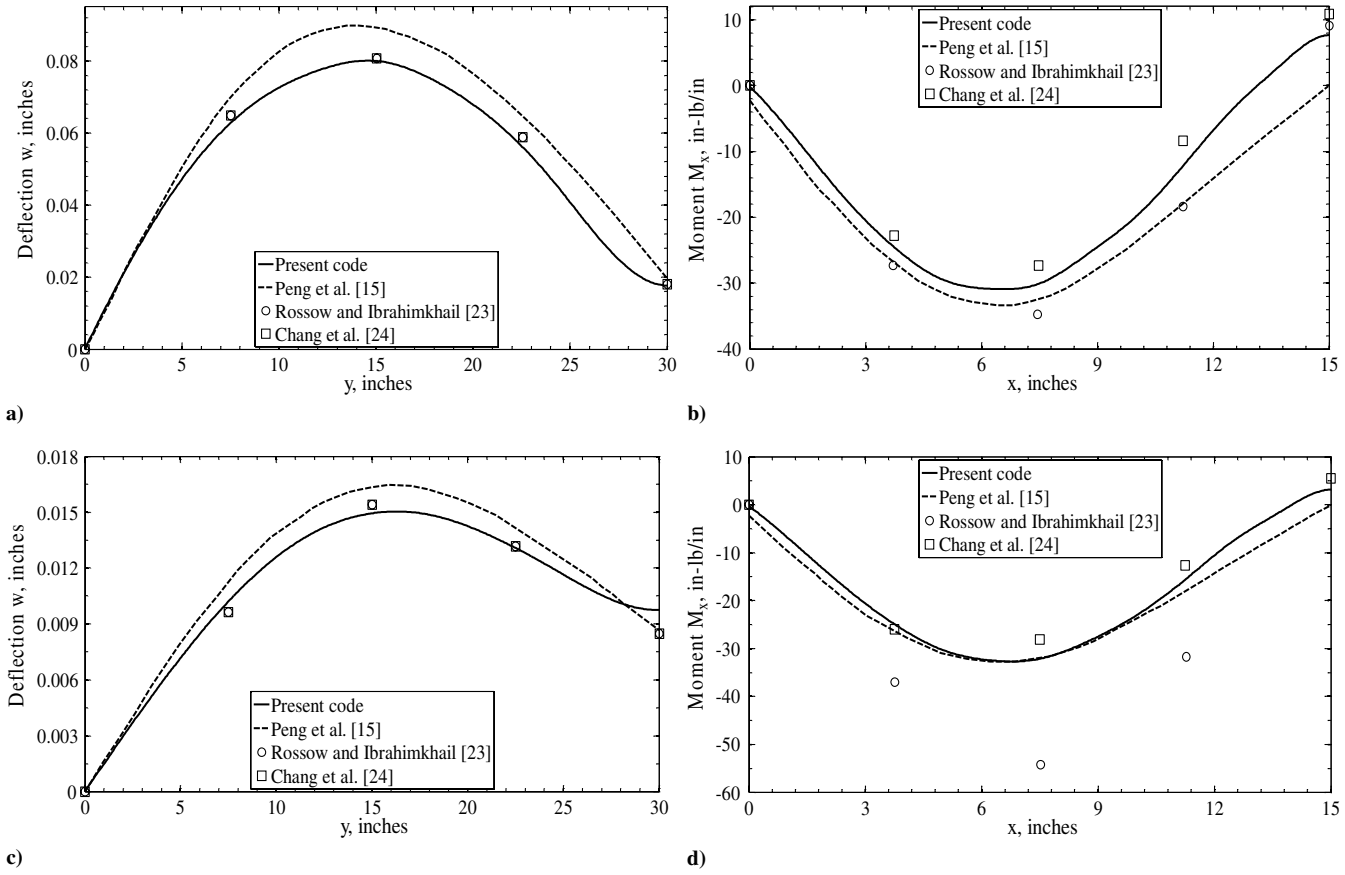

Fig. 12 Plots of a) deflection at $x = 7.5$ in., b) moment Mx at $y = 30$ in. (plate under distributed load is stiffened by concentric stiffeners), c) deflection at $x = 15$ in., and d) moment Mx at $y = 30$ in. (plate under distributed load is stiffened by eccentric stiffeners).

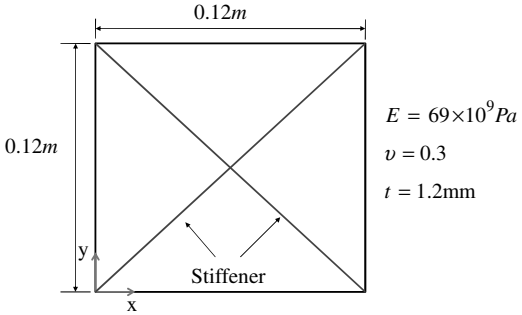

Fig. 13 Square plate with inclined stiffeners.

Mukherjee [8] solved this problem by using isoparametric stiffened-plate bending element. In their research, the stiffener can be positioned anywhere within the plate element. The plate and the stiffener are made of the same material, with Poisson's ratio $\upsilon = 0.3$. The buckling parameter is defined as

$$\lambda = \frac{\sigma_{cr} b^2 h_p}{\pi^2 D} \tag{30}$$

where σ_{cr} and D are the critical stress and the flexural rigidity of the plate. The ratio of the cross-sectional area of the stiffener to that of the plate is defined by $\delta = b_s h_s / b h_p$, where b_s and h_s are the width and the height of the stiffener. The ratio of the bending stiffness of the stiffener to that of the plate is defined by $\gamma = E_s I_s / bD$.

The accuracy of the present code is evaluated by considering the relative error and investigating the convergence. In ANSYS, the nodes of stiffener should match the nodes of plate; however, as has been mentioned before, in a mesh-free method, there is no need of having the particles of a stiffener and those of the plate to coincide. The relative error in the results given by this code with respect to a mesh-free scheme with 24×24 particles for the plate and 24 particles for the stiffeners is calculated. Also, convergence for the ANSYS results has been carried out. The relative error of the ANSYS is with respect to 24×24 nodes, and h is the distance between two particles and nodes in both the mesh-free method and ANSYS. For comparison, the numerically obtained convergence curve of mesh-free methods and ANSYS are compared and plotted in Fig. 6. From this figure, it can be seen that the mesh-free method has a better rate of convergence. The accuracy of mesh-free methods, as can be observed from the same figure, is also slightly better than ANSYS.

Table 1 shows the buckling parameter compared with the other results that are available in the literature [aspect ratio $(a/b) = 1$ and $GJ/Db_s = 0$]. It can be seen that there is a good agreement between the results of the present analysis and those that can be found in the literature. It is observed from this table that γ has an important effect on the buckling of the stiffened plate.

In the next step, the static analysis of the simply supported square plate with one stiffener at the center as shown in Fig. 7, is considered. The plate is subjected to a uniformly distributed load of 1.0 psi. The elastic moduli of both the plate and stiffener materials are the same: 17×10^6 psi. The Poisson ratio for both is 0.3.

This example was solved by Peng et al. [15]. They solved the problem by using EFG; however, in their formulation the stiffeners must be in x or y directions. This problem also has been solved by McBean [22] and Rossow and Ibrahimkhail [23] using the FEM. In the present formulation, since the stiffeners can possess any direction or curvature, they have more degrees of freedom than what Peng et al. [15] considered in their formulation. The results for eccentrically and concentrically stiffened plate are provided in Fig. 8. As can be seen in this figure, the results are close to what are available in the literature.

B. Simply Supported Plate with Two Stiffeners

A plate with two stiffeners and all edges simply supported analyzed by Timoshenko and Gere [1] and by Peng et al. [16] is selected as the second example. The geometry of the plate and the stiffeners are shown in Fig. 9. The plate is under uniaxial in-plane compression along the x direction. Parametric studies were conducted for plate aspect ratios (a/b). The buckling parameters obtained using mesh-free methods for $\delta = 0.05$ and $\gamma = 10/3$ are compared with other results in Fig. 10. As can be seen in this figure, the results are in good agreement with other available results.

The static analysis of the plate with orthogonal stiffeners has been conducted by considering the stiffeners in both concentric and eccentric configuration. The geometric and material properties of the stiffeners and the plate are shown in Fig. 11. The plate is subjected to a uniformly distributed load of 10.0 psi. The boundary conditions are taken to be simply supported. Peng et al. [15] solved this problem using EFG by considering straight stiffeners in the x or y directions.

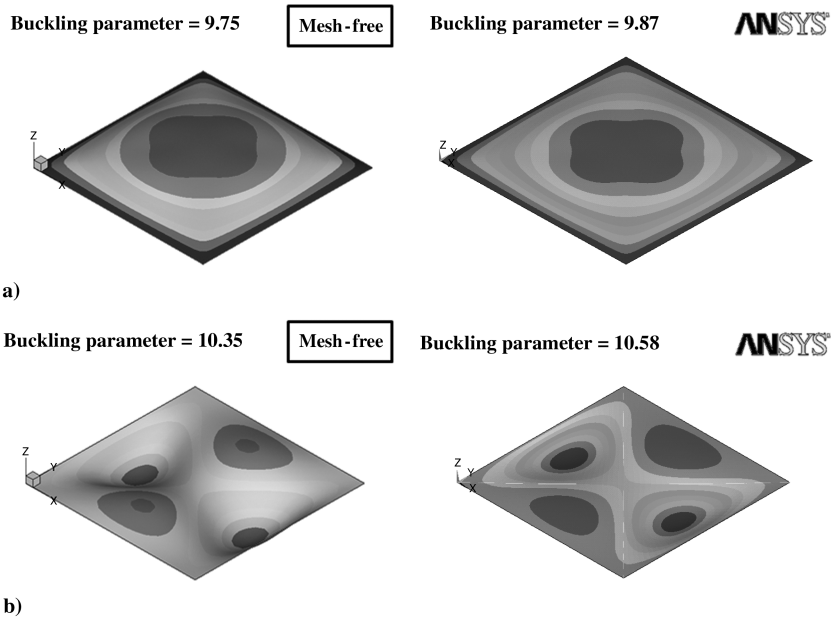

Fig. 14 Buckling mode shape for a plate with inclined stiffeners in biaxial compression using a mesh-free method (left) and ANSYS, a commercial available software (right): a) concentric stiffeners and b) eccentric stiffeners.

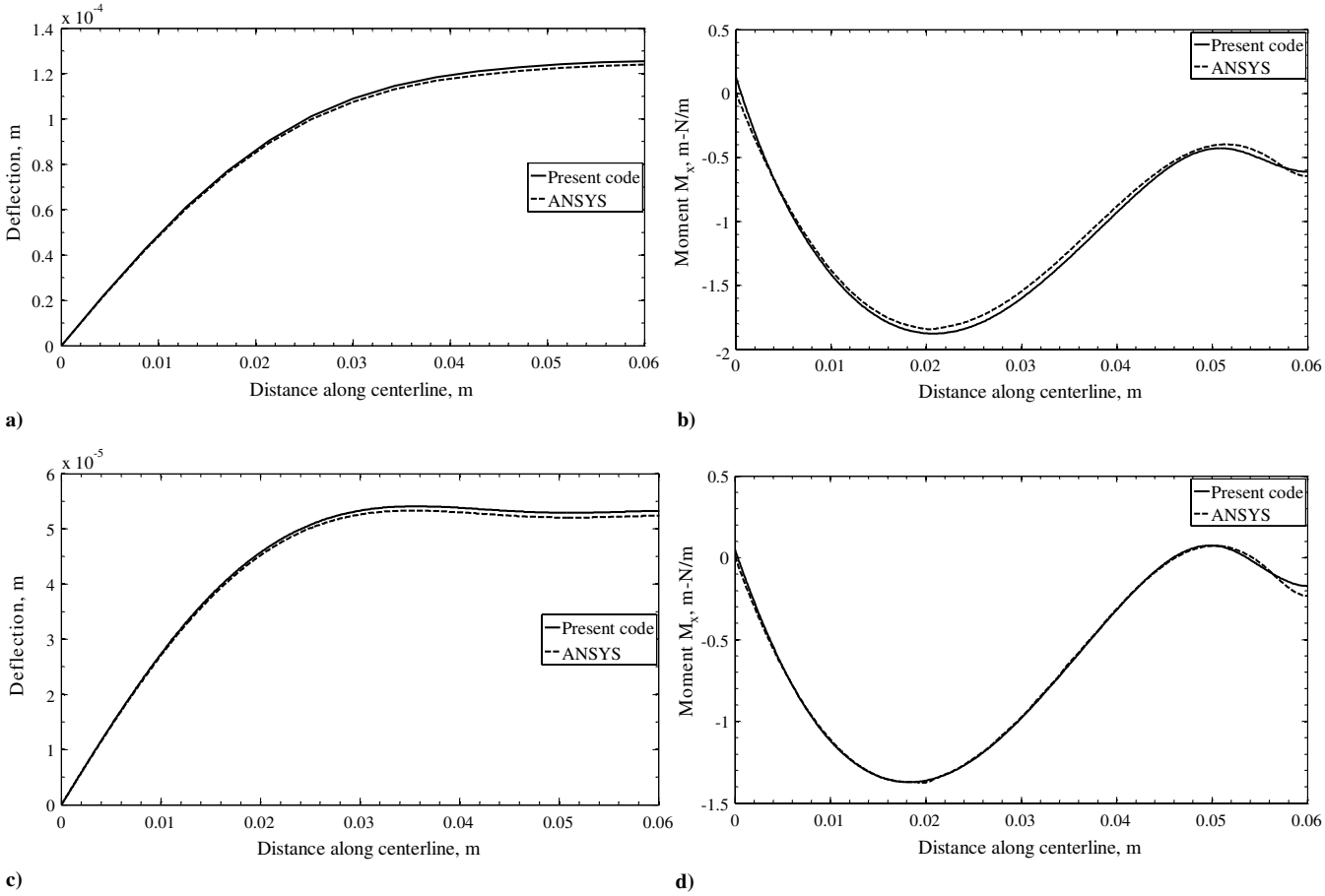

Fig. 15 Plots of a) deflection at $x = 0.06$ m, b) moment Mx at $y = 0.06$ m (plate under distributed load is stiffened by inclined concentric stiffeners), c) deflection at $x = 0.06$ m, and d) moment Mx at $y = 0.06$ m (plate under distributed load is stiffened by inclined eccentric stiffeners).

The problem was also solved by Rossow and Ibrahimkhail [23] and Chang [24]. The deflection along $x = 7.5$ in. for concentric stiffeners and $x = 15$ in. for eccentric stiffeners are shown in Fig. 12. The moments Mx for concentric and eccentric stiffeners along $y = 30$ in. are demonstrated in this figure. The deflection and moment agree closely with other available results. As can be seen, the agreement between the two sets of results for the concentric stiffeners is closer than that for eccentric stiffeners. This difference arises due to the differences between the plate and beam deformation theories, the method used in considering the effect of stiffener eccentricity in the stiffness matrix, and the differences in the shape functions used in the mentioned references and in the present paper.

C. Simply Supported Plate with Two Inclined Stiffeners

In this example, an eigenvalue analysis for determining buckling load is performed for the plate with inclined stiffeners subjected to biaxial compression. To check the accuracy of the present mesh-free code, results for inclined stiffeners are compared with those obtained using ANSYS. From the ANSYS library, 2250 SHELL63 and 100 BEAM188 are chosen for modeling the plate and stiffeners, respectively. The geometric and material properties of the stiffened plate are demonstrated in Fig. 13. In the mesh-free code, 22×22 particles and 60 particles are considered for the plate and stiffeners, respectively. The buckling parameters obtained for $\delta = 0.1$ and $\gamma = 10$ related to eccentric and concentric stiffeners. Accurate estimates of buckling parameters are achieved and the results are presented in Fig. 14.

In Fig. 15, deflections and bending moments per unit length are plotted along the centerline of the same plate when subjected to the distributed load of 10 kPa. Both concentric and eccentric stiffeners are considered in this example. Excellent agreement is observed. As might be expected, the eccentric stiffener can decrease both the stresses and the deflection of the plate.

D. Simply Supported Plate with a Curvilinear Stiffener

The next example considered in this study is the stability of a square plate with curvilinear stiffener subjected to biaxial compression. The stiffener configuration, plate geometry, and material properties are described in Fig. 16 ($\delta = 0.1$ and $\gamma = 10$). For comparison purposes, the complete stiffened plate was modeled in ANSYS with an irregular mesh composed of 2850 SHELL63 elements for modeling the plate and 60 BEAM188 elements for modeling each stiffener. Modeling a plate stiffened by curvilinear stiffeners in ANSYS needs a significant care in defining the stiffener geometry, since the stiffener elements must be placed along the mesh lines. In the mesh-free formulation, 24×24 particles and 40 particles are used to discretize the plate and the stiffener, respectively. In Fig. 17, it is clear that there is a good agreement between the buckling

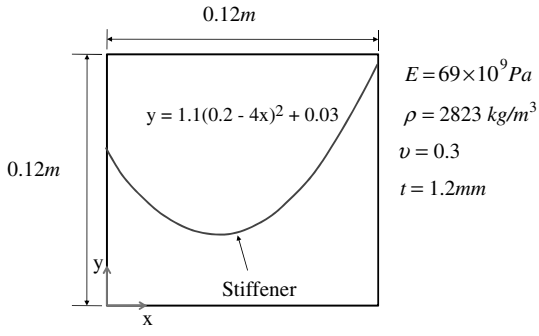

Fig. 16 Square plate with curvilinear stiffener.

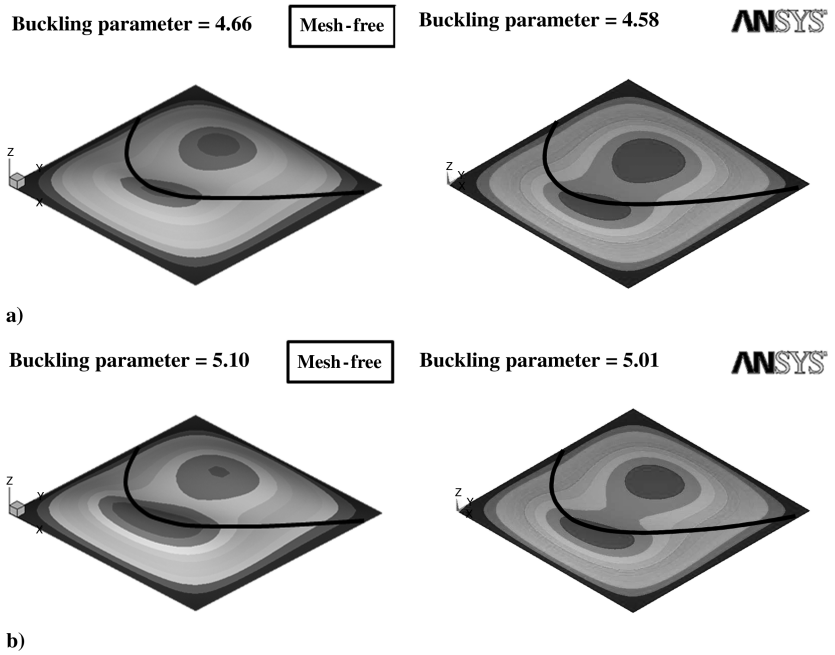

Fig. 17 Buckling mode shape for a plate with curvilinear stiffener in biaxial compression using a mesh-free method (left) and ANSYS, a commercial available software (right): a) concentric stiffeners and b) eccentric stiffeners.

parameters for a stiffened panel subjected to biaxial compression. The buckling mode shapes obtained using the mesh-free approach are similar to the buckling mode shapes obtained using ANSYS.

For static analysis, the simply supported plate with curvilinear stiffener, subjected to 10 kPa, is considered. The deflection results obtained using mesh-free methods, as can be seen in Fig. 18, agree well with those calculated using ANSYS. In ANSYS, the curvilinear stiffener is modeled by straight beam element and the stiffener nodes follow the plate nodes. The MLS shape function in the EFG method also enable us to predict more accurate results. The difference in the

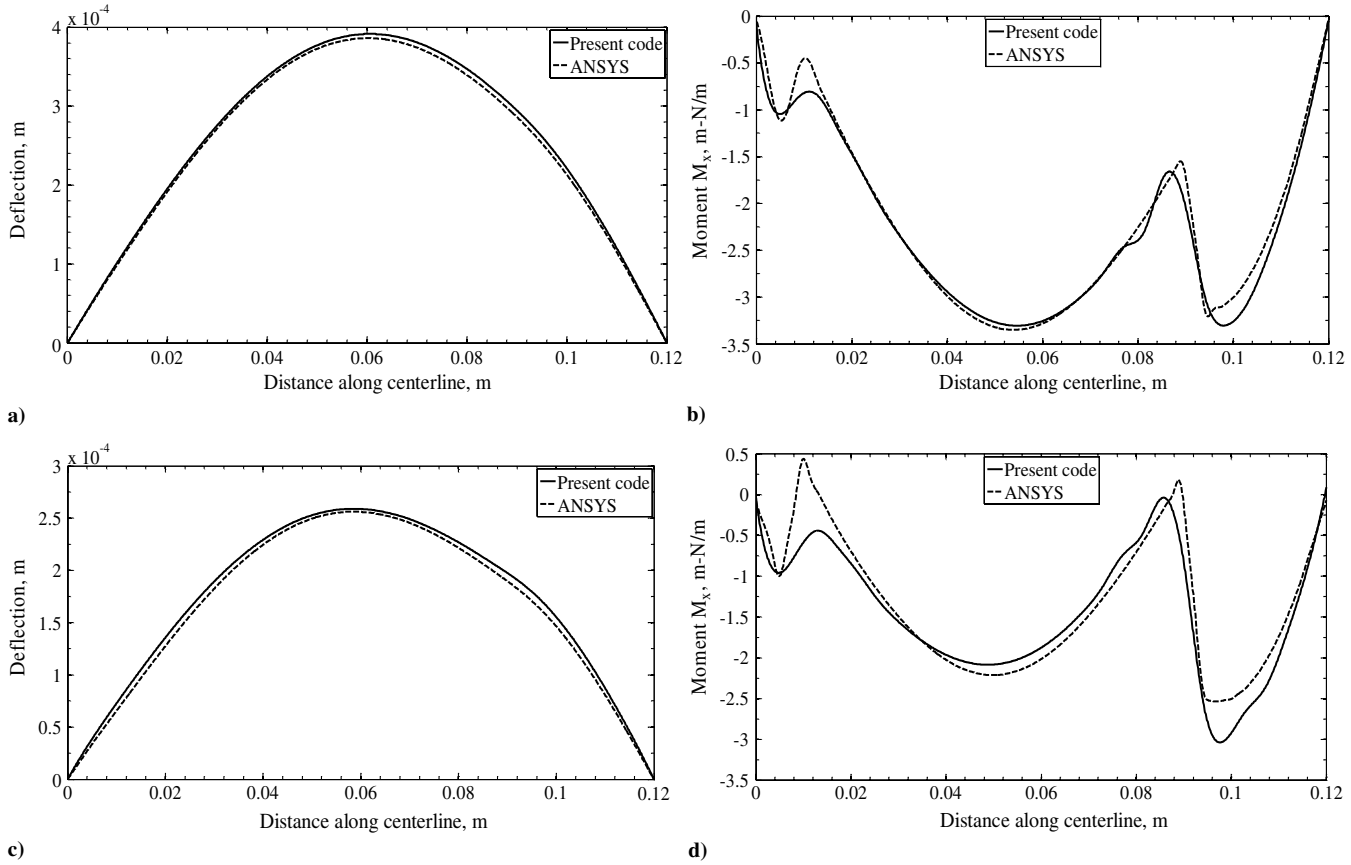

Fig. 18 Plots of a) deflection at $x = 0.06$ m, b) moment Mx at $y = 0.06$ m (plate under distributed load is stiffened by a concentric curvilinear stiffener), c) deflection at $x = 0.06$ m, and d) moment Mx at $y = 0.06$ m (plate under distributed load is stiffened by an eccentric curvilinear stiffener).

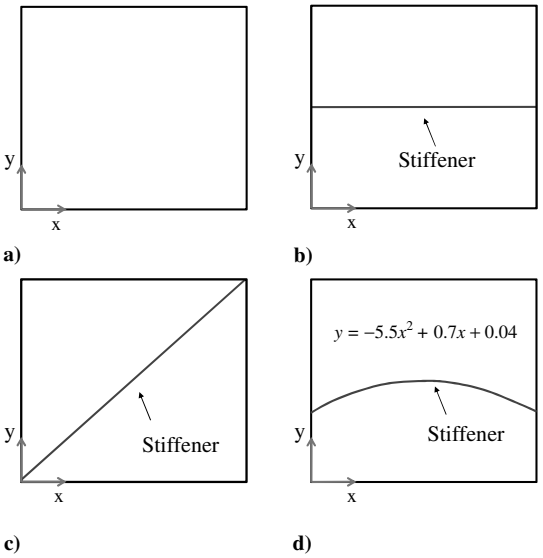

Fig. 19 Plots of a) unstiffened plate, b) plate with straight stiffener, c) plate with inclined stiffener, and d) plate with curvilinear stiffener.

moment results, especially for the eccentric stiffeners, may be due to the above reasons.

E. Simply Supported Plates with Different Stiffener Configurations

Square simply supported plates with different stiffener configurations are considered (Fig. 19) next. The plate is under a biaxial compressions and the material and the geometric properties are the same as in previous example. Three stiffener configurations are considered in this example; straight, inclined, and curvilinear. In previous examples, the results for these three configurations are compared with other methods. As we are interested in a high buckling parameter while having a low total mass, in this example, using the mesh-free method, both the buckling parameters and the masses of the unstiffened and the stiffened plates are compared. As can be seen in Table 2, the curvilinear stiffener can increase the buckling parameter,

$$\frac{\lambda_{\text{stiffened}} - \lambda_{\text{unstiffened}}}{\lambda_{\text{unstiffened}}} \times 100 = 165\%$$

while the total mass increases by a relatively small amount,

$$\frac{m_{\text{stiffened}} - m_{\text{unstiffened}}}{m_{\text{unstiffened}}} \times 100 = 10\%$$

As can be seen in Table 2, ANSYS is more efficient in terms of CPU time than the mesh-free code for the first analysis. However, it can be observed that as the stiffener shape changes while plate geometry properties are kept unchanged, the mesh-free code is more efficient in terms of CPU time than ANSYS. The final optimal design can be found by using optimization tools. As the stiffener configuration changes, the plate particles' locations in optimization' process need not to be modified. This gives a great capability in reducing the CPU time during optimization process.

In addition to changing the location or curvature of stiffener, adding another stiffener can increase the buckling parameter to a desired level while keeping the mass as minimum as possible. The buckling parameter and the mass of the plate with two stiffeners are shown in Fig. 20. By comparing Fig. 20 and Table 2, it can be seen that the buckling parameter increases significantly by adding the second stiffener. Consequently, the developed method can give the user the capability of changing the location, orientation, curvature, and number of stiffeners to find the buckling parameter, while the plate particles do not change.

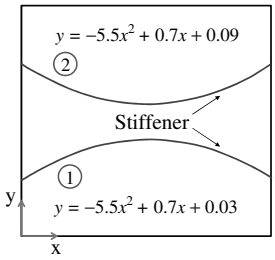

mass (kg)	0.0592
Buckling parameter	9.63

Fig. 20 Plate with two curvilinear stiffeners.

IV. Conclusions

The main objective of this study is to develop a mesh-free approach to analyze plates with arbitrary curvilinear stiffeners, and compare the accuracy with the results available in the literature. In the EFG method, employing the MLS basis functions, because the actual nodal values differ from the nodal parameters used in the MLS basis functions, boundary conditions cannot be imposed directly. The penalty method is used in this research to satisfy the boundary conditions. In this research linear buckling and static analysis are considered. The stiffener cross section is assumed to be symmetric about the stiffener binormal axis; however, the formulation accepts eccentric and concentric stiffeners. Accurate numerical results are obtained that not only are close to the results available in the literature but also to ANSYS results. In engineering design of stiffened plates, changing the stiffener properties and monitoring the structural behavior is one of the most important objects. In FEM modifying the stiffener location or curvature would lead to remeshing of the both plate and the stiffeners. However, in the present meshless formulation, because no mesh is required, remeshing the entire structure is avoided.

Appendix: Element-Free Galerkin Formulation for Buckling and Static Analysis of Stiffened Plate

The strain energy of the plate (U_p) and that of a stiffener (U_s) [19] are

$$U_p = \frac{1}{2}\delta_p^T \int_A B_p^T D_p B_p \, \mathrm{d}A \, \delta_p$$

$$U_s = \frac{1}{2}\delta_p^T T_{sp}^T \int_{-1}^{1} \Lambda^T B_s^T D_s B_s \Lambda \det J \, \mathrm{d}\zeta \, T_{sp} \, \delta_p \qquad \text{(A1)}$$

Matrices B_s, B_{Ns}, B_p, and B_{Np} for defining the plate and stiffener linear and geometric nonlinear strain vectors, in terms of nodal displacements vector, are

Table 2 Mass and buckling parameter of unstiffened and stiffened plates

	Unstiffened plate	Plate with straight stiffener	Plate with inclined stiffener	Plate with curvilinear stiffener (d)
Mass, kg	0.0488	0.0537	0.0557	0.0540
Buckling parameter (mesh-free)	1.98	5.07	5.05	5.25
Buckling parameter (ANSYS)	1.98	5.06	5.01	5.16
Time (mesh-free)[a]	1.6	1	1.1	1.1
Time (ANSYS)[a]	1.3	1.4	1.5	1.6

[a]Time is normalized.

$$[B_p]_i = \begin{bmatrix} \frac{\partial N_{pi}}{\partial x} & 0 & 0 & 0 & 0 \\ 0 & \frac{\partial N_{pi}}{\partial y} & 0 & 0 & 0 \\ \frac{\partial N_{pi}}{\partial y} & \frac{\partial N_{pi}}{\partial x} & 0 & 0 & 0 \\ 0 & 0 & N_{pi} & 0 & \frac{\partial N_{pi}}{\partial x} \\ 0 & 0 & 0 & N_{pi} & \frac{\partial N_{pi}}{\partial y} \\ 0 & 0 & \frac{\partial N_{pi}}{\partial x} & 0 & 0 \\ 0 & 0 & 0 & \frac{\partial N_{pi}}{\partial y} & 0 \\ 0 & 0 & \frac{\partial N_{pi}}{\partial y} & \frac{\partial N_{pi}}{\partial x} & 0 \end{bmatrix} \tag{A2}$$

$$[B_{Np}]_i = \begin{bmatrix} 0 & 0 & 0 & 0 & \frac{\partial N_{pi}}{\partial x} \\ 0 & 0 & 0 & 0 & \frac{\partial N_{pi}}{\partial y} \\ 0 & 0 & \frac{\partial N_{pi}}{\partial x} & 0 & 0 \\ 0 & 0 & 0 & \frac{\partial N_{pi}}{\partial y} & 0 \\ 0 & 0 & 0 & \frac{\partial N_{pi}}{\partial x} & 0 \\ 0 & 0 & \frac{\partial N_{pi}}{\partial y} & 0 & 0 \end{bmatrix}$$

$$[B_s]_i = \begin{bmatrix} \frac{1}{\det J}\frac{\mathrm{d}N_{si}}{\mathrm{d}\zeta} & \frac{N_{si}}{R} & 0 & 0 & 0 \\ -\frac{N_{si}}{R} & \frac{1}{\det J}\frac{\mathrm{d}N_{si}}{\mathrm{d}\zeta} & 0 & 0 & 0 \\ 0 & 0 & N_{si} & 0 & \frac{1}{\det J}\frac{\mathrm{d}N_{si}}{\mathrm{d}\zeta} \\ 0 & 0 & \frac{1}{\det J}\frac{\mathrm{d}N_{si}}{\mathrm{d}\zeta} & \frac{N_{si}}{R} & 0 \\ 0 & 0 & -\frac{N_{si}}{R} & \frac{1}{\det J}\frac{\mathrm{d}N_{si}}{\mathrm{d}\zeta} & 0 \end{bmatrix} \tag{A3}$$

$$[B_{Ns}]_i = \begin{bmatrix} 0 & 0 & 0 & 0 & \frac{1}{\det J}\frac{\mathrm{d}N_{si}}{\mathrm{d}\zeta} \\ 0 & 0 & \frac{1}{\det J}\frac{\mathrm{d}N_{si}}{\mathrm{d}\zeta} & \frac{N_{si}}{R} & 0 \\ 0 & 0 & -\frac{N_{si}}{R} & \frac{1}{\det J}\frac{\mathrm{d}N_{si}}{\mathrm{d}\zeta} & 0 \end{bmatrix}$$

The generalized stress–strain matrices for an isotropic material for plate and stiffener are

$$D_p = \frac{Eh_p}{1-\upsilon^2}\begin{bmatrix} 1 & & & & & & & \\ \upsilon & 1 & & & & & & \\ 0 & 0 & \frac{1-\upsilon}{2} & & & \text{sym.} & & \\ 0 & 0 & 0 & K_G\frac{1-\upsilon}{2} & & & & \\ 0 & 0 & 0 & 0 & K_G\frac{1-\upsilon}{2} & & & \\ 0 & 0 & 0 & 0 & 0 & \frac{h_p^2}{12} & & \\ 0 & 0 & 0 & 0 & 0 & \frac{\upsilon h_p^2}{12} & \frac{h_p^2}{12} & \\ 0 & 0 & 0 & 0 & 0 & 0 & 0 & \frac{h_p^2(1-\upsilon)}{24} \end{bmatrix}$$

$$D_s = \begin{bmatrix} E_sA_s & 0 & 0 & E_sA_s\bar{S} & 0 \\ 0 & G_sA_n & 0 & 0 & G_sA_s\bar{S} \\ 0 & 0 & G_sA_b & 0 & 0 \\ E_sA_s\bar{S} & 0 & 0 & E_sI_n & 0 \\ 0 & G_sA_s\bar{S} & 0 & 0 & G_sJ_t \end{bmatrix} \tag{A4}$$

The nodal displacements for plate and stiffener can be defined as

$$\delta_s = [u_{s1} \;\; v_{s1} \;\; \varphi_{sx1} \;\; \varphi_{sy1} \;\; w_{s1} \;\; \ldots \;\; u_{sN} \;\; v_{sN} \;\; \varphi_{sxN} \;\; \varphi_{syN} \;\; w_{sN}]^T$$
$$\delta_p = [u_{p1} \;\; v_{p1} \;\; \varphi_{px1} \;\; \varphi_{py1} \;\; w_{p1} \;\; \ldots \;\; u_{pn} \;\; v_{pn} \;\; \varphi_{pxn} \;\; \varphi_{pyn} \;\; w_{pn}]^T \tag{A5}$$

The linear elastic stiffness and geometric stiffness matrices and force vector are given as

$$K_p = \int_A B_p^T D_p B_p \,\mathrm{d}A + \alpha_p \int_{\Gamma_u} N_p^T N_p \,\mathrm{d}\Gamma$$
$$K_s = T_{sp}^T \int_{-1}^{1} \Lambda^T B_s^T D_s B_s \Lambda \det J \,\mathrm{d}\zeta \, T_{sp}$$
$$F = \int_{\Gamma_t} N_p^T f \,\mathrm{d}\Gamma + \alpha_p \int_{\Gamma_u} N_p^T \bar{u} \,\mathrm{d}\Gamma$$
$$K_{Gp} = \int_A B_{Np}^T \sigma_p B_{Np} \,\mathrm{d}A$$
$$K_{Gs} = T_{sp}^T \int_{-1}^{1} \Lambda^T B_{Ns}^T \sigma_s B_{Ns} \Lambda \det J \,\mathrm{d}\zeta \, T_{sp} \tag{A6}$$

Acknowledgments

The work presented here was funded under NASA Subsonic Fixed Wing Hybrid Body Technologies National Research Announcement NASA NN L08AA02C with Karen Taminger as the Associate Principal Investigator and Cynthia Lach as the Contract Officer Technical Representative. We are thankful to both Karen Taminger and Cynthia Lach for their suggestions. The authors would also like to thank our partners in the NRA project, Bob Olliffe, John Barnes, and Steve Englestadt, all of Lockheed Martin Aeronautics Company of Marietta, Georgia, for technical discussions. Additionally, the authors would like to thank the members of the Unitized Structure group. Thanks are also due to Institute for Critical Technologies and Applied Sciences at Virginia Polytechnic Institute and State University for providing laboratory space and other infrastructure.

References

[1] Timoshenko, S. P., and Gere, J. M., *Theory of Elastic Stability*, McGraw–Hill, New York, 1961.

[2] Seide, P., "The Effect of Longitudinal Stiffeners Located on One Side of a Plate on the Compressive Buckling Stress of the Plate Stiffener Combination," NASA TN 2873, 1953.

[3] Kolakowski, Z., "A Semi-Analytical Method for the Analysis of The Interactive Buckling of Thin-Walled Elastic Structures in the Second Order Approximation," *International Journal of Solids and Structures*, Vol. 33, No. 25, 1996, pp. 3779–3790. doi:10.1016/0020-7683(95)00211-1

[4] Byklum, E., Steen, E., and Amdahl, J., "A Semi-Analytical Model for Global Buckling and Postbuckling Analysis of Stiffened Panels," *Thin-Walled Structures*, Vol. 42, No. 5, 2004, pp. 701–717. doi:10.1016/j.tws.2003.12.006

[5] Brubak, L., Hellesland, J., and Steen, E., "Semi-Analytical Buckling Strength Analysis of Plates with Arbitrary Stiffener Arrangements," *Journal of Constructional Steel Research: JCSR*, Vol. 63, No. 4, 2007, pp. 532–543. doi:10.1016/j.jcsr.2006.06.002

[6] Bedair, O., "Discussion on Semi-Analytical Buckling Strength Analysis of Plates with Arbitrary Stiffener Arrangements by Brubak, J. Hellesland and E. Steen," *Journal of Constructional Steel Research: JCSR*, Vol. 63, No. 12, 2007, pp. 1616–1617. doi:10.1016/j.jcsr.2007.05.009

[7] Shastry, B. P., Venkateswara Rao, G., and Reddy, M. N., "Stability of Stiffened Plates Using High Precision Finite Element," *Nuclear Engineering and Design*, Vol. 36, No. 1, 1976, pp. 91–95. doi:10.1016/0029-5493(76)90145-X

[8] Mukhopadhyay, M., and Mukherjee, A., "Finite Element Buckling Analysis of Stiffened Plates," *Computers and Structures*, Vol. 34, No. 6, 1990, pp. 795–803. doi:10.1016/0045-7949(90)90350-B

[9] Biswal, K. C., and Ghosh, A. K., "Finite Element Analysis for Stiffened Laminated Plates Using Higher Order Shear Deformation Theory," *Computers and Structures*, Vol. 53, No. 1, 1994, pp. 161–171. doi:10.1016/0045-7949(94)90139-2

[10] Sadek, E. A., and Tawfik, S. A., "A Finite Element Model for the Analysis of Stiffened Laminated Plates," *Computers and Structures*, Vol. 75, No. 4, 2000, pp. 369–383. doi:10.1016/S0045-7949(99)00094-2

[11] Guot, Y.-L. and Lindner, J., "Analysis of Elastic-Plastic Interaction Buckling of Stiffened Panels by Spline Finite Strip Method," *Computers and Structures*, Vol. 46, No. 3, 1993, pp. 529–536. doi:10.1016/0045-7949(93)90222-Y

[12] Krysl, P., and Belytschko, T., "Analysis of Thin Shells by the Element-Free Galerkin Method," *Journal of Solids and Structures*, Vol. 33, No. 20, 1996, pp. 3057–3080.
[13] Atluri, S. N., and Zhu, T. L., "A New Meshless Local Petrov–Galerkin (MLPG) Approach in Computational Mechanics," *Computational Mechanics*, Vol. 22, No. 2, 1998, pp. 117–127. doi:10.1007/s004660050346
[14] Batra, R. C., and Zhang, G. M., "SSPH Basis Functions for Meshless Methods, and Comparison of Solutions with Strong and Weak Formulations," *Computational Mechanics*, Vol. 41, No. 4, 2008, pp. 527–545. doi:10.1007/s00466-007-0209-3
[15] Peng, L. X., Kitipornchai, S., and Liew, K. M., "Analysis of Rectangular Stiffened Plates Under Uniform Lateral Load Based on FSDT and Element-Free Galerkin Method," *International Journal of Mechanical Sciences*, Vol. 47, No. 2, 2005, pp. 251–276. doi:10.1016/j.ijmecsci.2004.12.006
[16] Peng, L. X., Liew, K. M. and Kitipornchai, S., "Buckling and Free Vibration Analyses of Stiffened Plates Using the FSDT Mesh-Free Method," *Journal of Sound and Vibration*, Vol. 289, No. 3, 2006, pp. 421–449. doi:10.1016/j.jsv.2005.02.023
[17] Kapania, R. K. and Li, J., "On a Geometrically Exact Curved/Twisted Beam Theory Under Rigid Cross-Section Assumption," *Computational Mechanics*, Vol. 30, Nos. 5–6, 2003, pp. 428–443. doi:10.1007/s00466-003-0421-8
[18] Kapania, R. K., and Li, J., "A Formulation and Implementation of Geometrically Exact Curved Beam Elements Incorporating Finite Strains and Finite Rotations," *Computational Mechanics*, Vol. 30, Nos. 5–6, 2003, pp. 444–459. doi:10.1007/s00466-003-0422-7
[19] Yeilaghi Tamijani, A., and Kapania, R. K., "Vibration of Plate with Curvilinear Stiffeners Using Mesh-Free Method," *AIAA Journal*, Vol. 48, No. 8, 2010, pp. 1569–1581. doi:10.2514/1.43082
[20] Zienkiewicz, O. C., *The Finite Element Method*, McGraw–Hill, New York, 1977.
[21] Zhu, T., and Atluri, S. N., "On a Modified Collocation Method and a Penalty Formulation for Enforcing the Essential Boundary Conditions in the Element-Free Galerkin Method," *Computational Mechanics*, Vol. 21, No. 3, 1998, pp. 211–222. doi:10.1007/s004660050296
[22] McBean, R. P., "Analysis of Stiffened Plates by the Finite Element Method," Ph.D. Thesis, Stanford Univ., Palo Alto, CA, 1968.
[23] Rossow, M. P., and Ibrahimkhail, A. K., "Constraint Method Analysis of Stiffened Plates," *Computers and Structures*, Vol. 8, No. 1, 1978, pp. 51–60. doi:10.1016/0045-7949(78)90159-1
[24] Chang, S. P., "Analysis of Eccentrically Stiffened Plates," Ph.D. Thesis, Univ. of Missouri, Columbia, MO, 1973.

R. Ohayon
Associate Editor